Electron Technology, 2, 2/3, pp. 53-66. Institute of Electron Technology P.A. Sci., Warsaw 1969

PRECISION LONG PATH INTERFEROMETRY AND THE VELOCITY OF LIGHT(1)

Precyzyjna interferometria dużych różnic dróg optycznych i szybkość światła

L'interférométrie de précision sur longues voies et la vitesse de la lumière

Прецизионная интерферометрия больших разностей хода и скорость света

J. L. HALL, R. L. BARGER, P. L. BENDER, H. S. BOYNE, J. E. FALLER(2), and J. WARD

Joint Institute for Laboratory Astrophysics(3)
Boulder, Colorado

WE REPORT here on several aspects of the JILA/NASA/NBS velocity of light experiment which has recently been started.

We discuss first the theory of the experiment and illustrate numerically that signal-to-noise ratio is not of primary concern. Considerable thought has gone into planning the experiment to be as free as possible from systematic error and these considerations will be briefly reviewed. We discuss a promising pair of laser transitions in pure neon and report two technological developments related to them. We will give a few illustrations of the kind of geophysical information that can be obtained from long-baseline interferometry of the type developed in this work. Finally we briefly report a useful laser transfer standard and a new wavelength reference based on laser saturation of a methane absorption line. A reproducibility of 3 parts in 10^{11} has already been demonstrated by optical heterodyne techniques in preliminary experiments.

The velocity of light experiment is based on the idea [1–4] of measuring the difference in frequency between a pair of closely-spaced gas laser lines, while simultaneously measuring the difference in wavelength with precision interferometric techniques.

In the work to be described, a pure neon laser oscillates on the doublet at 1.15 microns, producing two laser lines 51 GHz apart [5]. This beat frequency has already been measured in the laboratory [6]. The interferometic wavelength-difference measurements will be done in a 30 meter high finesse curved-mirror Fabry-Perot interferometer. For stability reasons the interferometer is evacuated and located in a remote unused gold mine located in the mountaines west of Boulder.

(1) Supported in part by NASA, Advanced Development Division, Goddard Space Center.

(2) Now at Weslyan University, Middletown, Conn.

(3) Of the National Bureau of Standards and the University of Colorado.

Let us consider first the wavelength measurement. For simplicity of presentation we will assume the path length such that we simultaneously have standing wave conditions for each line. Mirror phase shifts and other corrections will be treated later. Thus we have

$$N_1(\lambda_1)/2 = L, \; N_2(\lambda_2)/2 = L. \tag{1}$$

We can solve these for the (microwave) difference frequency $\Delta\nu$ between the two lines λ_1 and λ_2:

$$\Delta\nu \equiv \nu_1 - \nu_2 = c/\lambda_1 - c/\lambda_2, \qquad \Delta\nu = \frac{c}{2L}(N_1 - N_2). \tag{2}$$

The length L of the interferometer is very stable as will be seen later, but ultimately we will measure it optically in units of the stronger laser line. Calling this line λ_1, we can eliminate L from Eq. 2.

$$\Delta\nu = \frac{c}{\lambda_1}\left(\frac{N_1 - N_2}{N_1}\right), \tag{3}$$

or finally

$$c = \Delta\nu^* \lambda_1^* \frac{N_1}{N_1 - N_2}. \tag{4}$$

In our experiment $\Delta\nu \simeq 5.1 \times 10^{10}\ \mathrm{s}^{-1}$, $L = 30$ m, $\lambda \simeq 1.15\,\mu$m, $N_1 \simeq 5.3 \times 10^7$ and $N_1 - N_2 \simeq 10^4$.

To appreciate the power of this method, it is useful to calculate the total logarithmic derivative, $\delta C/C$

$$\frac{\delta c}{c} = \frac{\delta(\Delta\nu)}{\Delta\nu} + \frac{\delta\lambda_1}{\lambda_1} + \frac{\delta N_1}{N_1} - \frac{\delta(N_1 - N_2)}{N_1 - N_2}, \tag{5}$$

$$\frac{\delta c}{c} \simeq 10^{-8} \simeq 5\times10^{-10} + 5\times10^{-9} + 10^{-2}/5\times10^{7} + 10^{-4}/10^{4}. \tag{6}$$

The estimate for the frequency uncertainty is inferred from the measured residual instability of the optical frequencies themselves. The wavelength uncertainty represents the best published reproducibility with which laser wavelengths and krypton wavelength have been intercompared. It is essentially limited by the properties of the krypton lamp itself. We plan to measure the whole fringe number N_1, or equivalently, the whole optical path L, using a cluster of 5 or 6 laser lines near 1.15 μm. A precision, scanning method closely related to the "method of exact partial fringes" will be employed with successively greater etalon lengths, starting at a few cm. After a short etalon spacing is measured, the laser wavelength ratios are re-measured in it, and one "bootstraps" his way to 30 meters in 3 or 4 steps. The uncertainty in the whole fringe number N_1 is taken to be 1/100 of an order which is certainly conservative for a high finesse interferometer. One anticipates the major problem to be accurate measurement of the difference in fringe numbers, $N_1 - N_2$. We suggest 10^{-4} as a reasonable objective, leading to a probable error of 1×10^{-8} in the value to be obtained for the velocity of light. It is very important to distinguish at this point between *random* errors and *systematic* errors. Having the two laser lines closer together would require more care and more signal-to-noise ratio for a given precision.

However the important problems in high precision experiments are almost always the *systematic* effects. The concept of differential measurements between two quantities which are almost equal—and which consequently are treated almost equally by an apparatus—is one of the most powerful principles of experimental physics. Thus we anticipate a *sensitivity* loss rather than a loss of accuracy, corresponding to the smallness of the 2.26 Å separation of the two lines compared with the 11,500 Å basic wavelength. It is useful to treat this idea more quantitatively.

Let us collect mirror phase shifts, diffraction corrections, etc. into a small quantity ε for each wavelength

$$N_1 = N_1^0 + \varepsilon_1, \qquad N_2 = N_2^0 + \varepsilon_2; \tag{7}$$

N_1^0, N_2^0 are the integer fringe numbers we teach students about. The ε's are less than 1. Since $(N_1 - N_2) \ll N_1, N_2$ we are sure that an expansion of ε as a function of λ needs only a linear term, viz,

$$\varepsilon_2 = \varepsilon_1 + \frac{\delta\varepsilon}{\delta\lambda}\Delta\lambda. \tag{8}$$

In terms of the physical origins of ε, we can write

$$\begin{aligned} \frac{\partial\varepsilon}{\partial\lambda}\Delta\lambda = {} & \Delta \text{ (Dielectric Mirror Phase shift on reflection),} \\ & + \Delta \text{ (Diffraction correction),} \\ & + \Delta \text{ (wavefront sampling of interferometer plate figure).} \end{aligned} \tag{9}$$

Putting in appropriate numbers we get

$$\begin{aligned} \varepsilon_1 - \varepsilon_2 = \frac{\partial\varepsilon}{\partial\lambda} \times \Delta\lambda \simeq \frac{\frac{1}{2}\text{ order}}{1000\text{Å}} \times 2.2\,\text{Å} \quad & \text{phase shift,} \\ + (0.369 - 0.369) \quad & \text{diffraction correction.} \\ + \frac{(1/50)\,\text{wave}}{3\,\text{cm}} \times 0.5\,\text{cm} \frac{[\sqrt{\lambda_1} - \sqrt{\lambda_2}]}{\sqrt{\lambda_1}} \quad & \text{plate figure.} \end{aligned} \tag{10}$$

So

$$\varepsilon_1 - \varepsilon_2 = 10^{-3} + 0 + (1/3) \times 10^{-6} \tag{11}$$

and

$$\frac{(\varepsilon_1 - \varepsilon_2)}{N_2} = 10^{-7} + 0 + (1/3) \times 10^{-10}. \tag{12}$$

In the course of measuring the whole fringe numbers, the actual mirror phase shifts will be measured to about 1/100 order at 5 or 6 laser wavelengths ranging from 1.084 μm to 1.199 μm. Since the mirror reflectivity is a constant 99% over this whole band, it is expected that the phase will also be a slowly varying function over the wavelength range of interest. Thus an interpolation method should provide adequate accuracy, 10^{-4}, for the value $\varepsilon_1 - \varepsilon_2$.

It is an interesting property of single mode illumination of curved mirror interferometers that the diffraction correction is independent of wavelength [7]. Effectively the mode size scales appropriately with the wavelength $(\alpha\sqrt{\lambda})$ to produce the same diffraction effect and consequently the same geometrical mode, apart from the change in transverse

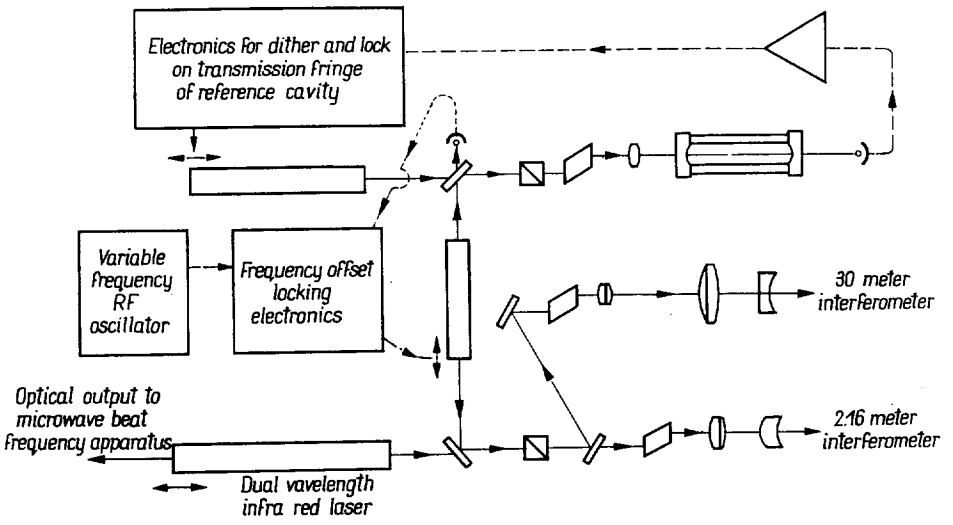

FIG. 1. Optical layout at Poorman's Mine. The use of two 6328 Å lasers and Frequency-Offset Locking allows the long interferometer to be well-stabilized at any convenient length. The auxiliary 2.16 meter path will be used in the determination of the whole fringe number. The Glan prisms and Fresnel rhombs provide reverse decoupling of $\geq 10^5$:1.

scale factor. The laser mode is similarly scaled. Thus a single optical transformation simultaneously matches both lines to the cavity.

We have seen that there does not appear to be any known difficulty which should in principle cause a systematic error equal to or greater than 1 part in 10^8. Whether or not this promise can be realized depends partly on signal-to-noise considerations. The laser to be described shortly produces about 25 microwatts, 20 of 1.15259 μm ($2S_2-2P_4$) and 5 of 1.15282 μm ($2S_4-2P_7$). The optical circuit from the laser through the interferometer should have a transmission of 1/20 or greater. This layout is illustrated in Fig. 1. Another beam splitter and solid etalon (λ_1, λ_2 filter) at the output lose an additional factor of 10 in the power. The noise-equivalent-power of available germanium photodetectors is around 2×10^{-12} watts for a 1 cps bandwidth. Thus we expect a working signal-to-noise ratio of

$$\frac{5\times10^{-6}\,\mathrm{W}}{2\times10^{-12}\,\mathrm{W}}\times\frac{1}{20}\times\frac{1}{10}>10^4{:}1.$$

We expect a finesse of at least 100 from the long interferometer now that the plates have been recoated to give $R = .99$ (theoretical finesse = 314). This high finesse is realistic in view of our mode-matching results with these plates. [A 6328 laser mode has been optically transformed so precisely into an eigenmode of the 30 meter cavity that only about

0.1% admixture of undesired modes was produced. Thus energy fed into the dominant mode should be effectively stored until ultimately dissipated by transmission through the mirror. Our 30 cm reference cavity used in the same manner has a measured finesse of 560!] With a linewidth of 1/100 order and a calculated signal-to-noise ratio of 10^4:1, we may reasonably expect to be able to split the fringes to 1%. As will be discussed shortly, stability of our environment is not a problem. Thus it appears that the velocity of light can be measured with these techniques with a probable error of the order of 1 part in 10^8.

It may be of interest briefly to mention some technological progress motivated by this velocity of light experiment. We have already reported [5] on a millimeter-wave apparatus useful in detecting and measuring the 51.36 GHz beat frequency between the two neon laser lines at 1.15 microns. The Schottky-barrier diode used has enough microwave sensitivi-

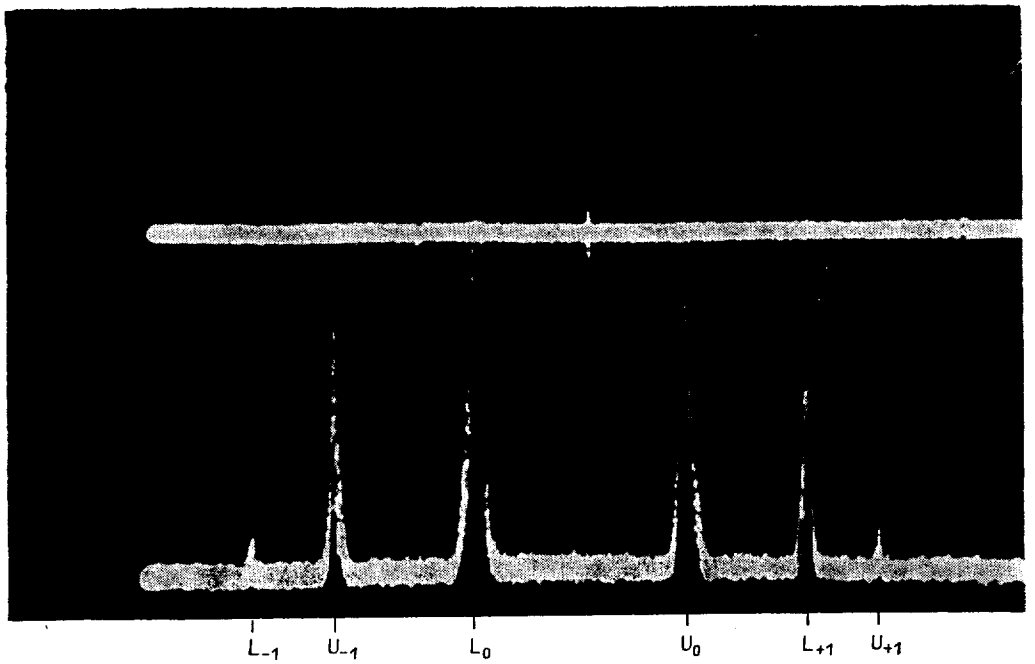

FIG. 2. Frequency swept display of *IF* amplifier output (lower trace). Upper trace shows (weak) heterodyne frequency marker at 51.36 GHz. Frequency scan is nonlinear due to klystron repeller characteristic.

ty *and* enough optical sensitivity to allow the two "tune-up" operations to be done independently. The diode also serves to heterodyne the 51.36 GHz with the 51.30 GHz klystron, producing thereby a 60 MHz output current. Figure 2 shows the spectrum resulting when the klystron frequency is swept. At this time the laser was oscillating in several longitudinal orders.

Soon after this work was reported we began work on the mode-suppressing three mirror system discussed by FOX and SMITH. This arrangement is illustrated in Fig. 3. In Fig. 4A only the mode-suppressor mirror is swept. The power output variations result as the reflectivity of the three-mirror system (viewed as a laser mirror) varies with its tuning. [The oscillation is largely constrained to be an axial mode of the longer inter-

ferometer due to its very high Q.] In this photo the single mirror at the far end was adjusted so that the "Lamb-dip" frequency is included in the comb of frequencies which are sequentially produced by scanning the mode-suppressor cavity. Figure 4B shows the envelope which results when the two cavities are asynchrously scanned. In Fig. 4C the mode--suppressor cavity is servo-locked so as to maximize the output power at each point in the (adiabatic) sweep of the oscillation frequency. Finally, in Fig. 4D, the long cavity

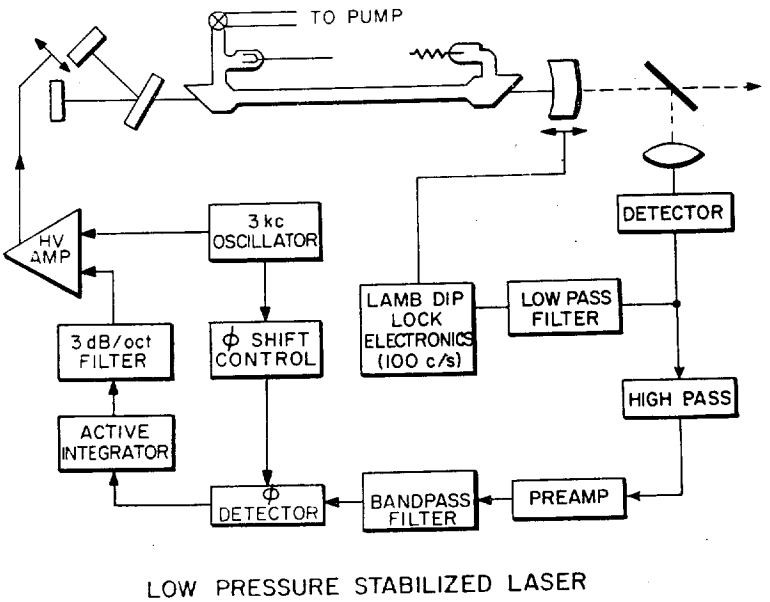

FIG. 3. Single axial-mode laser setup. Servo control of mode-suppressor cavity maximizes the output power. Servo control of the single mirror at the far end locks the laser frequency to the desired value, for example the Lamb-dip frequency.

is itself locked to the Lamb-dip. In the "C" experiment, this second lock will be to the 30 meter interferometer. Under the doubly-locked conditions illustrated in the figure, the spectral width of the single microwave beat frequency was too small to observe, the residual width ($\sim$ 1 KHz) being due primarily to ripple in the klystron power supply. Since then, the klystron has been phase-locked to a harmonic of a suitably stable 10 MHz oscillator, but the photobeat experiment has not yet been repeated with the improved apparatus.

We turn now to the interferometric stability experiments conducted over the last year or so at the Poorman's Relief Gold Mine. This mine is not now used for its intended purpose and instead has been partly refilled with concrete-and-steel piers, lasers, and electronics. Figure 5 shows the layout of the vacuum system, the three piers and the several bellows. Because of the bellows, the spacing between the piers is fixed by the solid granite rock, not by the aluminum tubing. Off to the left edge of the figure is the laser room, closed off about 7 meters from pier 1 by another partition. A control and electronics room, formerly used for storage of the high explosives used in hard-rock mining, is located about 30 meters from this second partition. The mine entrance is about 120 meters

beyond the control room. To reduce the influence of barometric pressure variations on the length of the 30 meter path, all of the otherwise unbalanced forces due to atmospheric pressure have been removed from the piers with auxiliary bellows and suitable anchors. One of the vertical supporting members for these bellows may be seen in Fig. 6, just beyond pier 2. The only side tunnel carrying fresh, moving air joins our tunnel about halfway between the laser room and the control room. When both doors of the laser room are closed to further restrict the air circulation, the resulting thermal and mechanical stability of this site is truly impressive. Our first observation, several years ago, showed drifts of

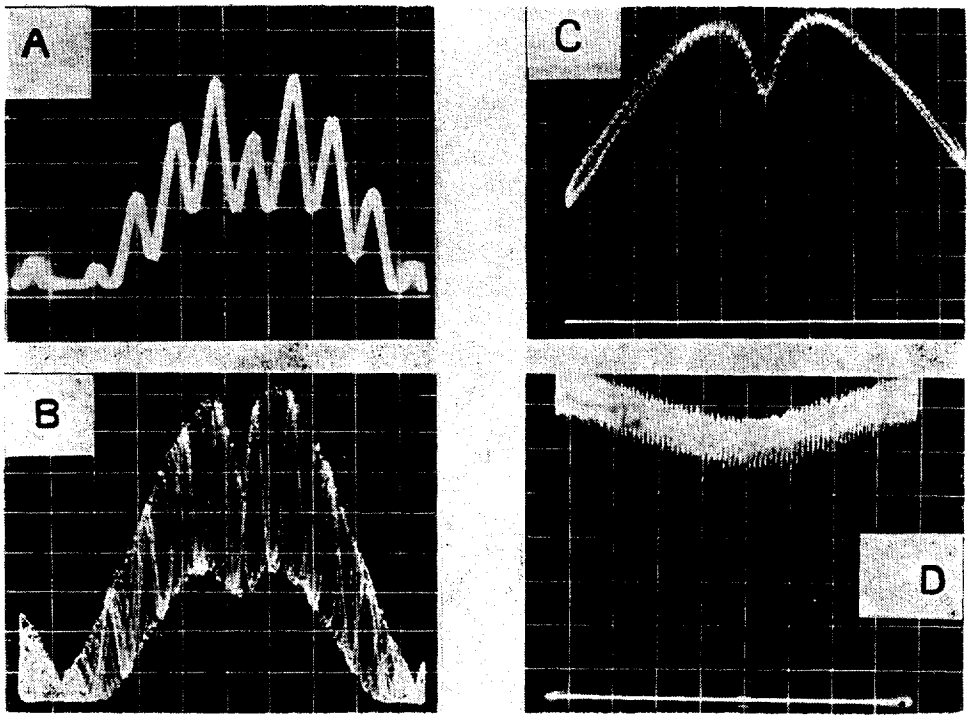

FIG. 4A. Apparatus of Fig. 3, operating at 1.15 μm in pure Ne^{20} at 0.15 Tr. Mode-suppressor mirror is swept. The length of the long cavity has been adjusted at the single mirror end to produce a comb of oscillation frequencies which includes the Lamb-dip frequency.

FIG. 4B. Both mirrors are driven, using incommensurable drive frequencies. All oscillating states are included in the envelope.

FIG. 4C. Output power vs tuning at the single-mirror end. The mode suppressor mirror is now servo-driven to produce the maximum output power at the frequency selected by the higher Q, long cavity.

FIG. 4D. Both servo loops operating, laser frequency modulated around the Lamb-dip and locked to it. The output power on this $2S_2-2P_4$ transition at 1.15 μm is about 20 μW, single frequency.

about 1 fringe (out of 10^8 fringes) per 5 minutes with an unstabilized 6328 Å laser. Since then, a fused quartz reference cavity with optically-contacted mirrors has been installed in a triple-walled, evacuated, constant temperature oven. (However it has not ever been necessary to servo-control the cavity temperature in this environment.) The cavity has a finesse of 560 and serves admirably as a sharp discriminator, having a full linewidth

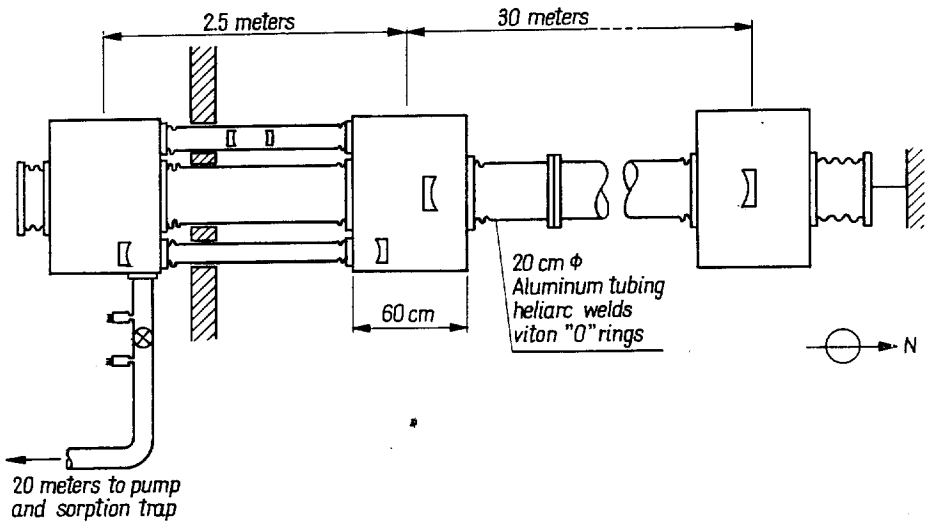

FIG. 5. Schematic of the vacuum system at Poorman's Mine. All heliarc welds have been helium leak-checked. At the 5 micron pressure reached by the mechanical pump, the whole fringe number N has been increased by 1 due to the residual gas.

FIG. 6. Standing in the doorway to the laser room, looking north along the 30 meter interferometer. The lefthand vacuum tube (with the feedthrough insulators) contains the 30 cm reference cavity; the optical path of the 2.16 m interferometer passes through the righthand tube. The vertical poles anchor the barometric-pressure relief bellows. At the 9°C ambient temperature, moisture condensation can be appreciable in the springtime.

of only 0.8 MHz. An RF excited, stable 6328 Å laser is locked to this cavity. With this stable wavelength as its input, the 30 meter interferometer is then locked to the peak of its transmission fringe. The optical system illustrated in Fig. 1, and presently being constructed, will allow the long interferometer to be stabilized at any convenient length or scanned in a precisely-known manner.

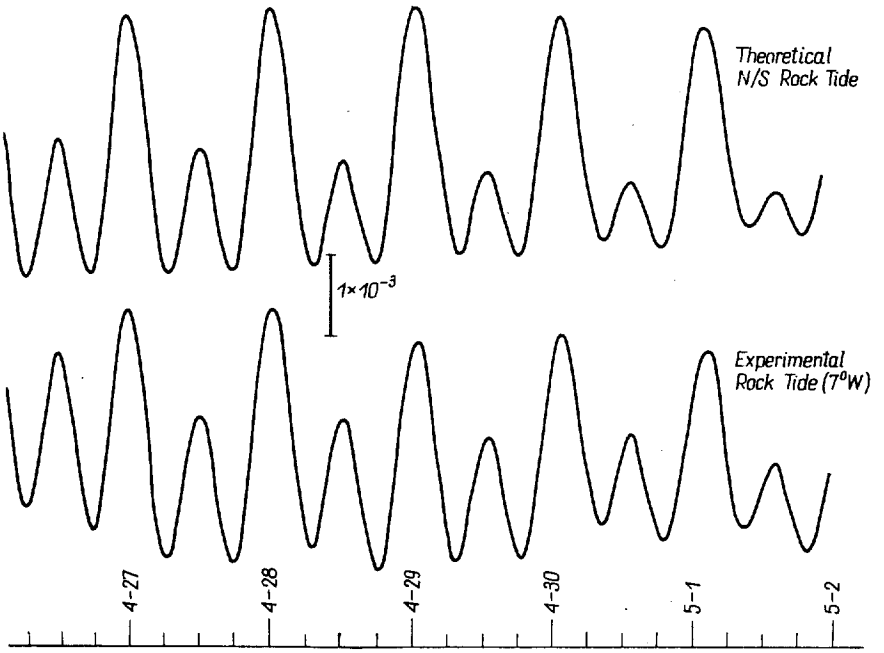

FIG. 7. Earth tide data for the period April 26 through May 2, 1968. The lower (experimental) curve has been replotted by hand to remove the 1 fringe steps generated by the automatic ranging circuit. The upper (theoretical) curve contains only the tide amplitude as a free parameter.

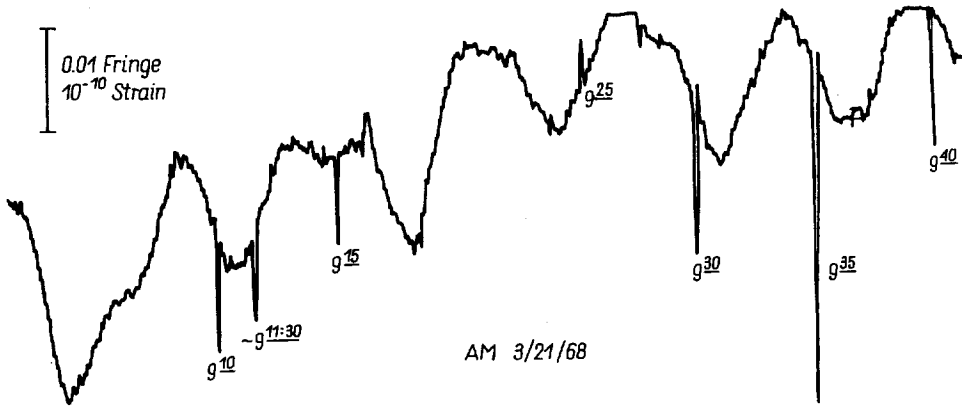

FIG. 8. Quiet interval around 9 a.m. on March 21, 1968. The data have been smoothed about a factor of 3 by a digital filter of 3 s averaging time. The oscillations with a period ~ 5 min may be of barometric rather than seismic origin. The general upward trend is due to the earth tide being displayed at such high magnification.

Due to good mechanical design of the piers and mirror mounts, the long path error signal (fed to its electrostrictive ceramic elements to control the length to be precisely constant) may be regarded as a measure of earth strain. Thus we see gravitational tides in the earth's crust of up to 5 fringes amplitude. About 1 week of such data is illustrated in the lower half of Fig. 7. [The actual recordings have jumps of one fringe generated by the automatic range apparatus—for clarity these have been removed.] The upper half of the figure is a computer-synthesized theoretical rock tide at our location, calculated for the pure north-south strain component [10]. The fact that our interferometer turns out actually to lie about 7° west of north probably accounts for the difference in the second-harmonic component. These data in comparison with the theoretical tides well illustrate the excellent long-term stability of this environment. The apparent drift of the *system*, of the order of 1 in 10^9 per week, corresponds to a 2 millidegree change in the temperature of the reference cavity if the entire change is assigned to this source.

On a shorter time scale, Fig. 8 shows the "relatively typical" quiet interval. The higher frequency components have been smoothed by a factor of 3 or so with a digital filter of

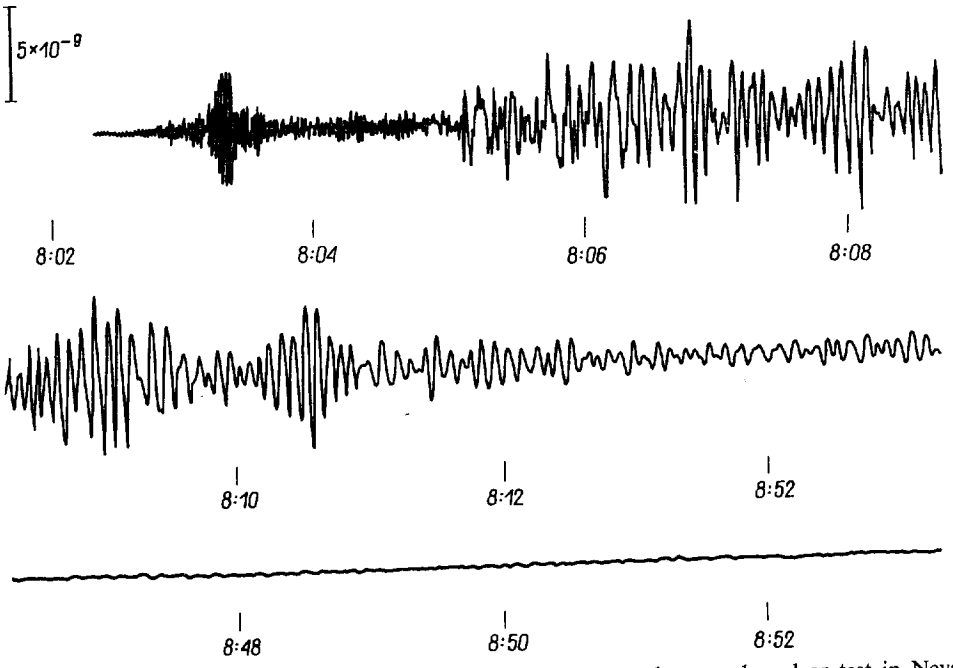

FIG. 9. Arrival in Boulder of a seismic disturbance related to an underground nuclear test in Nevad

3 seconds averaging time. Drift rates of 2 or 3 in 10^{11} per minute seem to be typica The general upward trend is due to the earth tide being displayed at such high magnific tion. On such a quiet day this residual noise, a few hundredths of a fringe or so, is d to microseism activity. The microseism spectrum, measured by other methods, peaks a few seconds/cycle. The oscillations with a period $\sim$ 5 minutes may be of barometri rather than seismic, origin. The observed signal-to-noise ratio of $\sim$ 50 : 1 thus sets

upper limit of 10^{-11} for electronic and optical system noise. From the point of view of the velocity of light experiment, these variations of the order of a fringe or less are the open loop error signal. With small input errors and good signal-to-noise ratio, the length servo should be very effective in producing an ideal, fixed-length Fabry-Perot spacer.

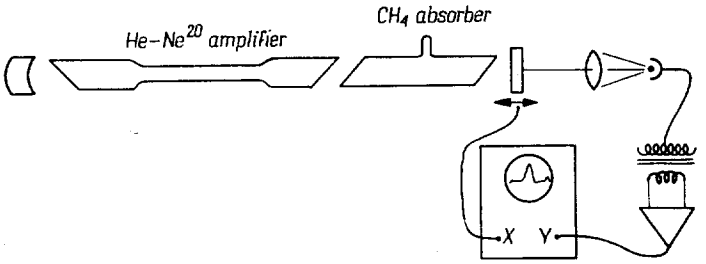

FIG. 10. Saturated Molecular Absorption Apparatus. The 1 mW output at 3.39 μm of the He-Ne laser corresponds to about 1 W/cm² inside the cavity.

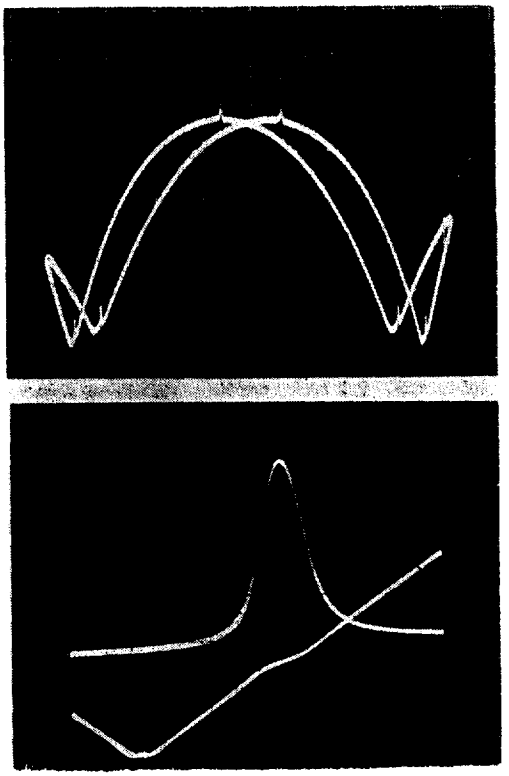

FIG. 11. Upper Photo: Output power vs laser cavity tuning. Only the upper 20% of the 1 mW output is displayed full scale. The cavity scan axis is 28 MHz/division. The saturation peak is about 2% amplitude and 400 kHz wide at half height. At ~ 12 Tr the Ne^{20} laser has been pressure-shifted into good coincidence with the CH_4 absorption line. Lower Photo: Upper trace—similar to above, except cavity tuning scale is 2 MHz/division. Lower trace is output of wideband, linear frequency-to-voltage converter displayed against the same cavity scan as the upper trace. Note the "frequency hangup" near line center as the oscillation frequency is strongly pulled by the methane resonance.

For general interest, we include Fig. 9. It shows the error signal due to the arrival in Boulder of a seismic disturbance related to *a* nuclear explosion detonated underground in Nevada. Our pre-arrival noise level was not approached within a factor of 3 for many hours.

The general conclusions seem to be that a), lasers and long-path interferometry will be useful in geophysics, and b), with relatively modest effort we should be able to servo our path-length to be as constant as we need.

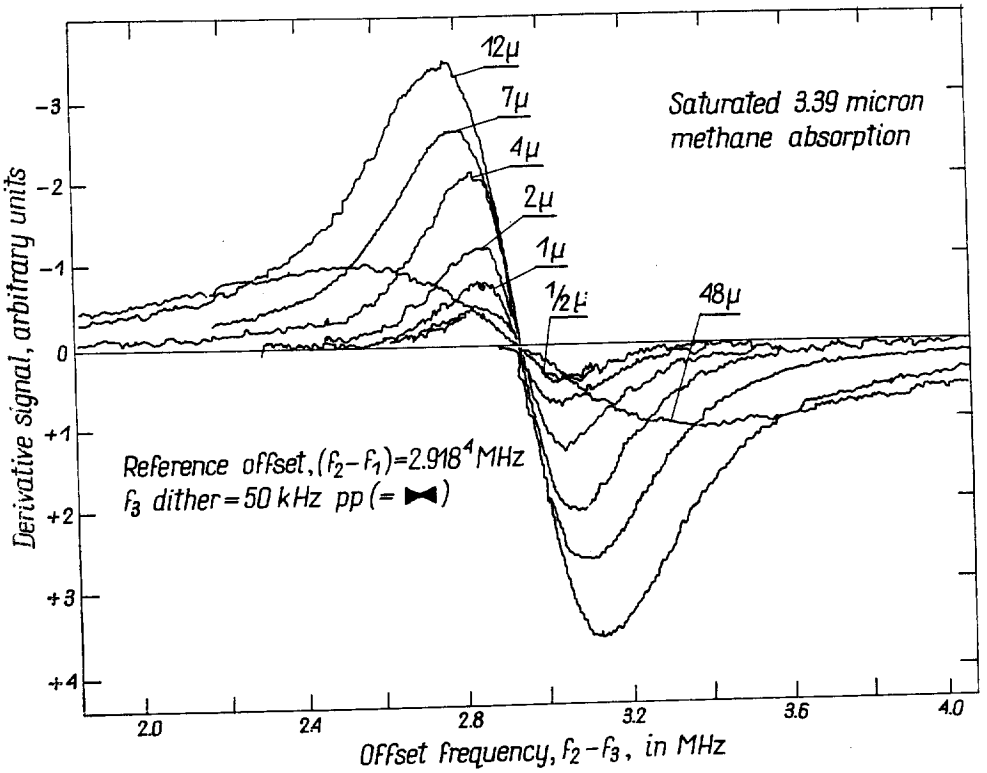

FIG. 12. Derivative of output power with respect to frequency, plotted versus frequency. Line center corresponds to where the f_2-f_3 beat frequency is equal to the f_2-f_1 reference frequency of 2.9184 MHz. The frequency for which the derivative is zero is remarkably insensitive to methane pressure over the range 1/4 to 48 μm.

Finally, we report two laser devices which should prove useful in precision metrology. The first is the pure neon laser, oscillating on the 1.15259 micron transition ($2S_2-2P_4$), which has an anomalously small pressure shift [11]. An independent reproducibility of better than $1:10^9$ has been demonstrated. This laser has high gain and a very low operating pressure. It can give a highly useable stabilized output for less than 10 watts system power input and thus should find additional application as a portable high-precision transfer standard. By good luck, this line is also the stronger of our beat-frequency pair. Thus heterodyne comparisons of wavelength can easily be done at the mine to measure

the long term drifts. Eventually it may be used to transfer the standard krypton centimeter up to the mine. More discussion and results may be found in Ref. [11].

The second laser device promises to be fundamental wavelength standard of the highest quality and utility. The idea [11] is to study the sharp natural absorption line of a suitable molecule by partially saturating its absorbing transition with a laser. Those molecules having only transverse thermal velocity components interact (strongly) with both cavity running waves. The resulting partial saturation of the molecules having zero axial velocity thus reduces the interacavity opacity, giving rise to an "emission" feature precisely at line center. The apparatus is illustrated in Fig. 10. Our first work exploits the unique stability of a methane vibration-rotation line at 3.39 microns wavelength, excited by the helium-neon laser transition ($3S_2-3P_4$) [12]. In Fig. 11 we show that the wavelength

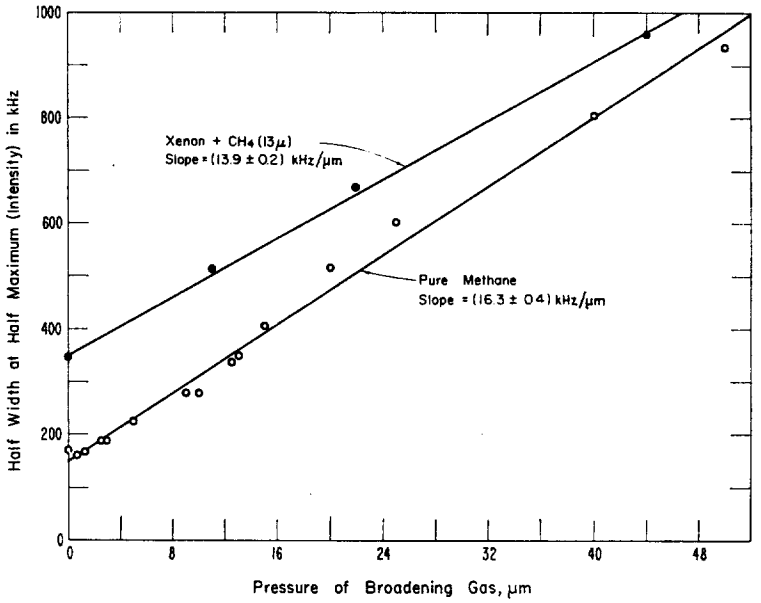

FIG. 13. Linewidth of the Lorentz saturation feature at half-maximum intensity. The same pressure scale applies to both xenon and methane as the collision-broadening gas. In the xenon runs, the methane pressure was 13 μm.

coincidence may be made very good by a suitable pressure-shift of the Ne^{20} transition. With the technique of "Frequency-Offset Laser Locking", we are able to scan the resonance with extreme stability. Figure 12 shows the variation of the derivative-with-respect--to-frequency of the output power. The lack of a pressure-shift is clear from these analogue data. We are presently unable to reliably measure the pressure shift, even with excellent digital data and computer lineshape analysis, the interim best value being (75 ± 150) Hz/μm. The beat frequency between two independently-stabilized devices was (2.6 ± 2) kHz. To our knowledge, this demonstrated reproducibility of better than $3:10^{11}$ is better by 1 1/2 orders of magnitude than any optical results previously reported. In addition to its use as a potential wavelength standard, this concept should allow investigation of gas-phase collision effects with a sensitivity never before available [13].

REFERENCES

1. P. L. BENDER, Radio Science, **68D**, 523, 1964.
2. Z. BAY and H. S. BOYNE, School of Physics "Enrico Fermi", 31 Course, 1964.
3. C. K. N. PATEL and W. M. SHARPLESS, Proc. IEEE, **52**, 107, 1964.
4. W. R. BENNETT, Jr. and J. W. KNUTSON, Jr., Proc. IEEE, **52**, 861, 1964.
5. J. L. HALL and W. W. MOREY, Appl. Phys. Lett., **10**, 152, 1967.
6. K. D. MIELENZ, K. F. NEFFLEN, W. R. C. ROWLEY, D. C. WILSON and E. ENGELHARD, Appl. Opt., **7**, 289, 1968.
7. G. D. BOYD and M. KOGELNIK, Bell System Tech. Jour., **41**, 1347, 1965.
8. Hewlett Packard Associates, Palo Alto, Calif., type 2350.
9. A. G. FOX and P. W. SMITH, J. Quantum Electr., **1**, 343, 1965.
10. These calculations were made by J. WARD using a computer program similar to the one kindly made available by Dr. J. C. HARRISON (Geological Sciences Dept. of the University of Colorado).
11. J. L. HALL, *The Laser Wavelength Standard Problem*, 5th International Conference on Quantum Electronics, Miami, Fla., May 1968. To appear in the J. Quantum Electr., October 1968.
12. K. SHIMODA, *Absolute Frequency Stabilization of the* 3.39 *Micron Laser on a* CH_4 *Line*, paper presented at the Conference on Precision Electromagnetic Measurements, Boulder, Colorado, June 1968.
13. Our very interesting but still preliminary results on line-shape studies and absolute resettability will be published later.